Computational Condensed Matter 9 (2016) 6–12

Contents lists available at ScienceDirect

Computational Condensed Matter

journal homepage: http://ees.elsevier.com/cocom/default.asp

Steps roughening in thermal relaxation and low-coverage growth of sloped Pt(110) and Ir(110) surfaces: A numerical study

S.I.V. Hontinfinde [a], R.A. Yessoufou [a, b], F. Hontinfinde [a, b, *]

[a] Département de Physique, Université d'Abomey-Calavi, Benin
[b] Institut de Mathématiques et de Sciences Physiques, Dangbo Université de Porto-Novo, 01 BP 613, Porto-Novo, Benin

ARTICLE INFO

Article history:
Received 19 June 2016
Received in revised form
2 August 2016
Accepted 3 August 2016
Available online 7 August 2016

Keywords:
Monte Carlo simulations
Sloped Pt and Ir (110) surfaces
Step width and roughness
Adatom and island densities
Power-law behavior

ABSTRACT

The dynamical roughening of [001] steps on sloped Pt (110) and Ir (110) surfaces is investigated by kinetic Monte Carlo simulations. Our model includes deposition, diffusion and fully reversible aggregation on these surfaces with both anisotropic barriers and anisotropic attachment. The barriers for the diffusion processes have been calculated by means of classical molecular dynamics simulations where both metals are modeled by realistic many-body potentials. The roughness is evaluated through calculations of the step width in thermal relaxation of the surface and low-coverage growth conditions. Results indicated a non-trivial behavior of the width in time during relaxation. In growth, power-law behavior is recovered for both metal surfaces. Defects population on terraces is investigated through calculations of adatom and island densities. It is found that at very low temperature (T = 200K for Pt and 400K for Ir and below), a power-law behavior with the growth time is got. Beyond, fluctuations in generated data become important and do not allow to correctly access the true trend of both quantities. Their behavior with the diffusion length at low temperature is singled out.

1. Introduction

In the past three decades, much effort has been devoted to control the evolution and the morphology of crystal surfaces in epitaxial growth of materials [1–3]. It has been established that mass transport through surface diffusion is an essential ingredient since it provides the efficient microscopic smoothening mechanism required to grow atomically flat surfaces for technological applications. In particular, the role of interlayer diffusion in determining the surface morphology has been a subject of much theoretical and experimental works [4,5]. Results indicated that the existence of a barrier to step-descent can lead to morphological instability with mounds, ripples or facets formation [6–8]. The average size and the spatial separation of the latters were found to increase with growth time. Less is however known about epitaxial growth of vicinal surfaces that are natural supports for nano-objects. They have interesting properties that are used in catalysis and growth of components for electronic devices [9–11]. In suitable growth conditions, growth of these surfaces may proceed via steps propagation [12]. In others, islands may nucleate and grow on terraces and this systematically destroys the step-flow mode. During the growth, steps naturally interact. The interaction potential is believed to be of the form [13,14]: $V(l) = A/l^2$, l is the terrace width and A the interaction constant. Estimation of the terrace width distribution (TWD) has been an attracting subject of fundamental research since it gives relevant informations on the nature of step-step interactions [15,16]. Fewer works focused on step roughening on stepped surfaces in epitaxial growth and this mainly motivated the present investigation. Also statistics of islands, kinks, adatoms, etc on terraces of vicinal (physical) surfaces are almost lacking in the literature while a huge number of works focused on this problem on high-symmetry surfaces in epitaxial growth [1,17].

In this paper, we address these problems on two stepped surfaces: Pt (110) and Ir (110) surfaces by means of realistic kinetic Monte Carlo simulations (KMC). These surfaces have rectangular symmetry and can show missingrow reconstruction structures. They have also different stabilities in the sense that Pt (110) surface stabilizes through (111) facets whereas Ir (110) surface stabilizes through (331) facets. It has been demonstrated that the existence of the leapfrog diffusion mechanism for dimers or atomic chains diffusion on these surfaces, plays a crucial role in their stabilization

* Corresponding author. Département de Physique, Université d'Abomey-Calavi, Benin.
E-mail address: fhontinfinde@yahoo.fr (F. Hontinfinde).

http://dx.doi.org/10.1016/j.cocom.2016.08.001

[18]. Here, we study the kinetic roughening of parallel steps along the [001] direction, ie steps normal to the atomic rows. Relevant diffusion events include both intralayer and interlayer processes. Associated barriers have been calculated by means of quenched molecular dynamics simulations [19,20] where both metals are modeled by many-body potentials derived within the second moment approximation to the tight-binding model [21]. The steps roughening during thermal surface relaxation and submonolayer growth is investigated through an anisotropic bond-breaking model (ABBM) [17, 19, 20]. Beyond that, adatom and island densities on terraces in the submonolayer regime have been computated. During relaxation or growth, we find that steps roughen in a non-trivial way. At very low temperature, adatom and island densities show a power-law behavior with the growth time. When the temperature increases, the behavior looks different. In particular, we get that island density behaves linearly with the growth time.

In Section II, the model and the simulation procedure are described. In Section III, our results are presented. Section IV is devoted to concluding remarks.

2. Model and simulation

Diffusion processes relevant to the surface growth or relaxation are summarized in Fig. 1a [17,19,20]. They include atom hopping by jump along the [110] direction (process p_1); atom exchange in the [001] direction (process p_2); atom detachment from steps or islands by the breaking of one (as in the Figure), two or three bonds with nearest-neighbors (process p_3) and step descent (process p_4); dimer diffusion by leapfrog mechanism is included in the model (process p_5). Corresponding energy barriers are given in Table 1 for both metal surfaces. Here, due to the structure of the samples under investigation (see Fig. 1a), we do not consider metastable atomic walks [22] that may be important on (2×1) missing-row reconstructed Pt(110) surfaces. Atomic bonds along the [110] and [001] will be respectively referred to as parallel and normal bonds. They cost 0.36 eV and 0.03 eV for Pt (110) and 0.53 eV and 0.03 eV for Ir(110) respectively.

Energy barriers E_p and E_n for atom diffusion along [110] and [001] directions are respectively calculated using the ABBM. The ABBM is based on two assumptions. For a given diffusion process, the energy barrier is based only on the environment of the diffusing atom in the initial position. Second, the barrier of the diffusion process can be computed adding contributions from in-channel (parallel) and cross-channel (normal) bonds to the barrier for the diffusion of an isolated adatom. Then, the barrier for a given process is written in the form:

$$E_p = E_p^0 + n_p E_p^b + n_n E_n^b, \tag{1}$$

$$E_n = E_n^0 + n_p E_p^b + n_n E_n^b \tag{2}$$

where E_p^0/E_n^0 Is the barrier for single atom hopping along the [110]/[001] direction; n_p/n_n denotes the number of parallel/normal bonds to be broken by the diffusing atom; and are bond energies along [110] and [001] respectively. The diffusion rates are of Arrhenius type:

$$D_{p,n} = \nu \times \exp(-E_{p,n}/kT), \tag{3}$$

where $E_{p,n}$ is the activation energy barrier for the diffusion process calculated using the previous formulae. The prefactor ν is invariably set to 10^{12}sec^{-1}. Particles are deposited on the surface with a flux F. Landed on non-equilibrium sites, atoms will funnel down to nearby growth sites.

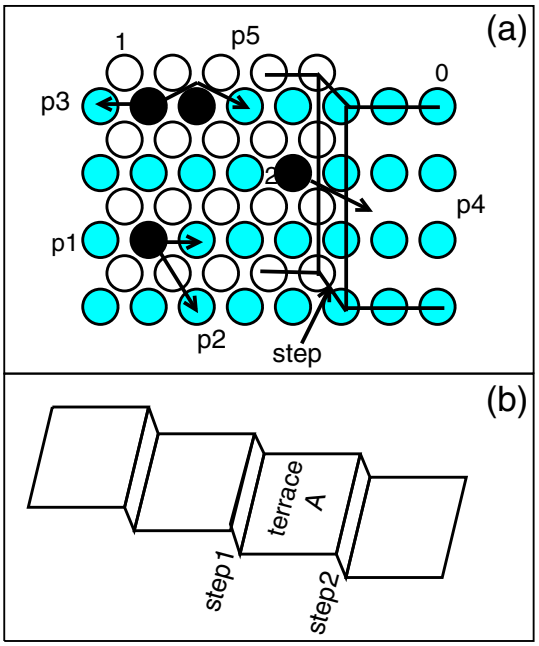

Fig. 1. Inlayer and interlayer diffusion processes relevant to Pt and Ir (110) surfaces epitaxial growth (panel a) and a schematic representation of sloped Pt and Ir (110) surfaces (panel b). In panel (a), process p_1 is associated to atom hopping in the in-channel direction, process p_2 to cross-channel exchange diffusion, process p_3 to atom detachment from island or step, process p_4 to step-descent move in the in-channel direction, and process p_5 to leapfrog atom diffusion. Black atoms are at level 2, white atoms at level 1 and grey atoms at level 0. In panel (b), a terrace A limited by two descending and ascending steps is shown.

The simulation algorithm considered here has been used to study Ag (110) high-symmetry surfaces in several previous works and yielded interesting results consistent with experimental findings (see [23, 24]). Here, Pt and Ir (110) sloped surfaces with parallel steps oriented in the [001] direction are considered (Fig. 1b). Atoms are deposited on these substrates at a flux F. Diffusion processes happen with rate D. KMC simulations with the Bortz, Kalos and Lebowitz (BKL) algorithm [25] are used. A move is performed at each step according to its a priory probability. For a configuration C obtained at a given step of the simulations, the total evolution rate

$$R_c = F + \sum_k \nu_k exp(-E_{p,n}/kT) \tag{4}$$

is computated as well as its real lifetime $\tau = -\log(r)/R_c$ where r is a random number between 0 and 1. Then, a random number r_1 is selected and the random rate $Q_c = r_1 \times R_c$ calculated. By summing rates of possible processes of configuration C, the process $k = b$ such that the condition:

$$F + \sum_k \nu_k exp(-E_{p,n}/kT) \geq Q_c \tag{5}$$

holds is realized with probability 1. Processes of the new configuration are updated and the total evolution rate recalculated. After a

Table 1
Energy barriers (in eV) for relevant diffusion processes on Pt(110) and Ir(110) surfaces diplayed in Fig. 1a.

Process	*p*1	*p*2	*p*3	*p*4	*p*5
Pt(110)	0.60	0.80	0.96	0.64	0.84
Ir(110)	1.22	1.60	1.75	1.27	1.68

certain simulation time period t where Ω new configurations are generated, values of quantities of interest are estimated by a time-averaging procedure.

3. Results and discussions

The stepped surface schematized in Fig. 1b is considered. Each lattice consists of 128 × 64 sites. Samples with 128 × 48 sites generate similar results. Thus, finite-size effects on the following results could be neglected. Periodic boundary conditions at the lattice edges are imposed on atomic heights in the [001] direction. In the [110] direction, diffusion ocurs by jumps while in the [001] direction it preferentially happens by exchange as indicated in Fig. 1a. Our statistics are obtained on two selected consecutive steps (eg. steps limiting terrace A in Fig. 1b) and values of computated quantities are averaged over 10^2 to 2.10^3 independent runs. We first calculate steps width as a function of real relaxation time t in the absence of external atomic flux (F = 0mL/sec) by using step profiles given by lines connecting centres of step atoms. Then, the step roughness is quantified by computing the usual step width W. A terrace with a descending step at its edge is mapped onto a 2D-dimensional crystal where the descending step atoms represent a 1D surface atoms with well-defined heights. By means of this mapping, a step width W is calculated by the usual formula:

$$W = (1/L)\sum_i \left(h_i - \overline{h}\right)^2 \tag{6}$$

where $\overline{h}$ is the 1D surface mean height and h_i is the height of a step (or surface) atom at position i. This quantity is shown in Fig. 2 for both metals as a function of the real simulation time t at selected values of the absolute temperature. It ressorts that results for Pt (110) are still noisy after averages over two thousands independent runs. Both steps of terrace A show approximately the same roughness at the considered temperature (open triangles and circles). The step width W behaves neither logarithmically with time nor as a power-law. The two full lines of each panel are related to these two trends obtained by regression. One remarks that at the early stage of the relaxation process, W nearly scales as a power-law with time, but this power-law fitting completely fails in the course of the time. One remarks that computed data are almost fully enclosed by the two fitting curves in each panel. Such behavior has been somewhat observed with Au(110) and Ag(110) at low temperature in recent numerical calculations [26]. Therefore, a combination of a logarithmic and a power functions in the form:

$$\frac{1}{2}\left(\lambda_0 + \lambda_1 log(t) + \lambda_2 t^{\lambda_3}\right) \tag{7}$$

may approximately describe the steps width for both metals in the early stage of the epitaxial growth process. For three selected temperatures, fitted values of λ_1 and λ_3 for one selected step of terrace A are given in Table 2. Let us remark that the exponent λ_3 decreases with increasing temperature whereas λ_1 is increasing; this means first that thermally activated diffusion processes are playing an important smoothening role. Second, a logarithmic kinetic roughening is expected for all steps at high temperature.

In the non-equilibrium case, the behavior of W is displayed in Fig. 3a,e as a function of the absolute temperature at different simulation times given by the numbers (written on the curves) of atoms deposited on the substrate. We use the experimental atomic flux F = 1 mL/min. One sees for both metal surfaces that the steps roughness develops in time in a nontrivial way. Different curves show two inflexion points as the temperature is increased. The first one may be associated to the onset of surface diffusion processes on the substrate. Below this inflexion point (onset temperature), fluctuations of step profiles should be essentially caused by atoms that land directly at step edges. In-channel diffusion that represents the fastest diffusion process becomes active from this onset and drain landed adatoms to moving steps which become rougher and rougher. The second may be related to the onset temperature for atom detachment processes from steps and islands. This generates a huge number of adatoms that eventually diffuse to steps since surface diffusion become more and more important in the dynamics. This explains why the step width W increases sharply from the second onset temperature. For 512 atoms deposited, the first onset is obtained at T = 290K and the second one at 340K for Pt(110) while for Ir(110), one gets T = 560K and T = 680K. Let us remark that onset temperatures for Ir(110) are almost the double of those estimated for Pt(110). This results from the relation that exists between energy barriers for diffusion processes on both metal surfaces. Snapshots of sections of step profiles are displayed in other panels. It is interesting to remark that the barrier of in-channel diffusion on Ir(110) is approximately twice its value on Pt(110). This holds also for the cross-channel diffusion as well as for the leapfrog diffusion and step descent move. Therefore, one may expect to get the same kinetic roughening of steps at temperature T for Pt(110) and at temperature 2T for Ir(110), eg. at T = 400K and T = 800K. Unfortunately, this is not the case. At any time in the submonolayer regime, steps on Ir(110) surface appear rougher with more fluctuations as it can be seen by comparing snapshots (b-d) and (f-h). The reason may be related to the fact that in-channel bond breaking on Ir(110) at 2T costs less in the dynamics than at T for Pt(110). Therefore, before the second onset temperature for Ir(110), W (T) on Pt(110) should similarly behaves as W (2T) on Ir(110) surfaces. By analyzing how values of W at fixed temperatures change with the number of deposited atoms in panels (a) and (e), one can conclude that these values may be linked to each other

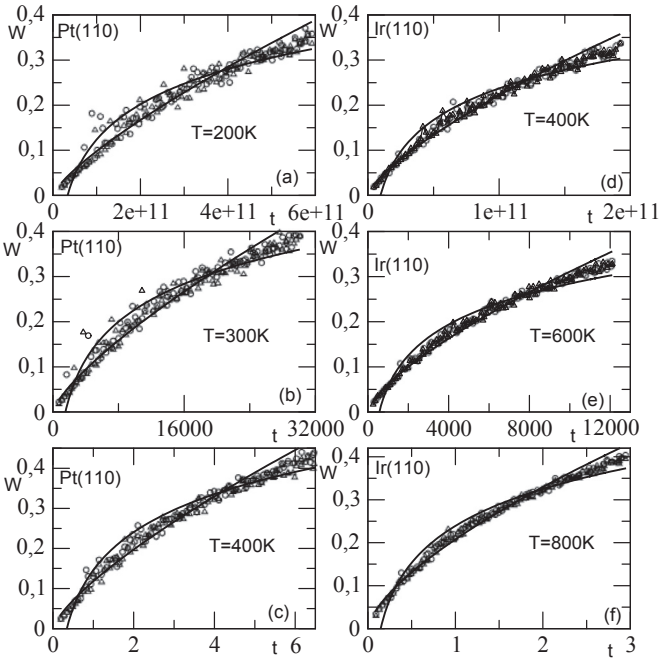

Fig. 2. Width of two consecutive steps as those shown in panel (b) of Fig. 1 for Pt(110) surface (left panels) and Ir(110) surface (right panels) and selected values of the temperature at zero atom deposition flux. Two full data fitting lines (logarithmic and power curves) are displayed. The very early time data are best-fitted to a power function. Beyond, data should be correctly described by a combination of both functions (see text).

Table 2
Fitted values of λ_1 and λ_3 for P t(110) and Ir(110) surfaces.

Surface	T (*K*)	λ_1	λ_3
Pt(110)	200	0.113 ± 0.004	0.770 ± 0.019
	300	0.121 ± 0.003	0.751 ± 0.015
	400	0.137 ± 0.003	0.741 ± 0.013
Ir(110)	400	0.101 ± 0.002	0.730 ± 0.009
	600	0.103 ± 0.002	0.705 ± 0.08
	800	0.124 ± 0.003	0.665 ± 0.007

Fitted values of this exponent are displayed in Table 3. From these results, one may conclude that the time exponent β decreases with temperature at fixed deposition flux. At very low temperature several curves collapse stating that surface diffusion is still playing a very minor role at fixed F. Contrarily to the previous behavior of W, we note that the deposition flux increases the step roughness. This appears evident from results displayed in Table 4

Adatom and island densities are also characterized on terraces. Many experiments have been performed in the past to study

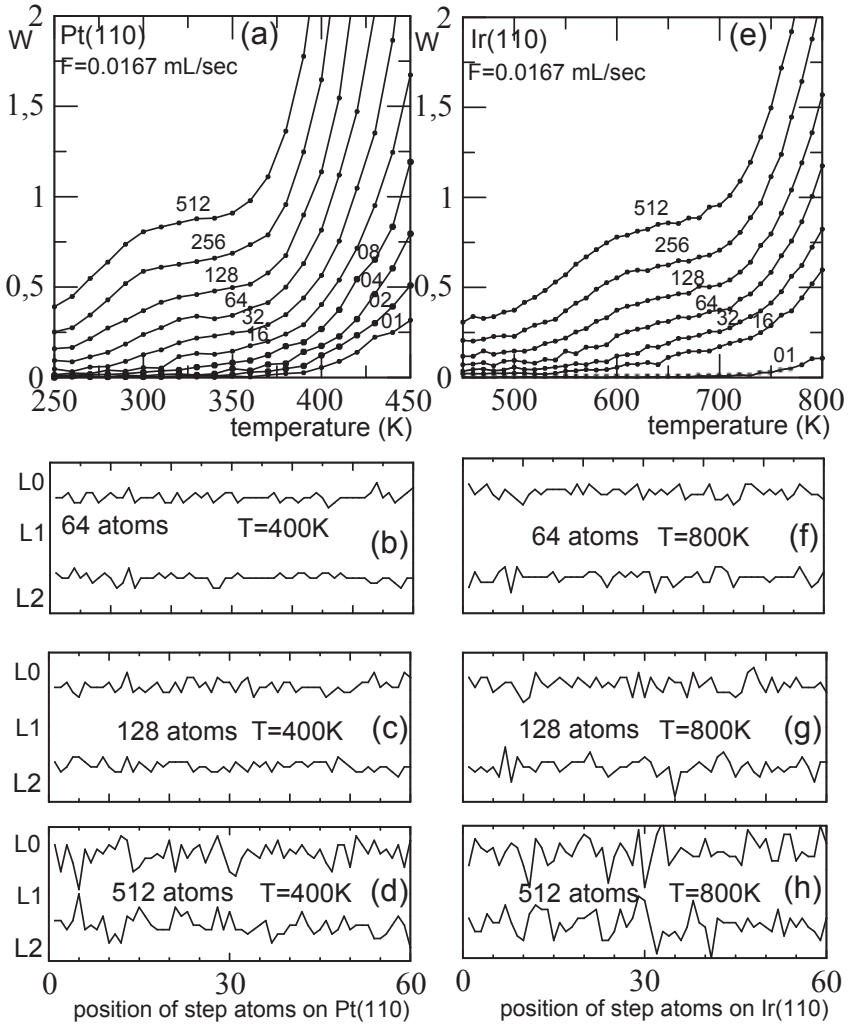

Fig. 3. Step widths at the experimental flux of 1 mL/min at different simulation times as functions of the absolute temperature T for Pt (110) surface (panel a) and Ir (110) surface (panel e). The corresponding step profiles at two selected temperatures are presented for both metal surfaces. Terrace levels are denoted by L0 (level 0), L_1 (level 1) and L2 (level 2).

by an interesting relation. Intuitively, we plotted in a log-log scale, at selected values of the temperature (see Fig. 4), W as a function of the number of deposited atoms. We recall the readers that the latter is related to the real simulation time t through values of the atomic flux. Right panels are associated to Ir(110) and left panels correspond to Pt(110). From the top to the bottom, panels correspond to increasing values of the deposition flux. We find through all panels that the early stage behavior of W could be fitted to linear curves. This suggests a power-law behavior of W (t). After a certain time period which depends on the values of the atomic flux, the temperature and the nature of the substrate, the straight fitting lines change slopes in most cases. Let us somewhat describe what happens in the two last panels of Fig. 4. There, one can write $W(t) \sim t^{\beta}$.

morphologies of aggregates on crystal surfaces that simulated much theoretical work. These experiments were analyzed by rate equations theory [27, 28] and Monte Carlo simulations [1,17,19] to predict monomer and island densities as well as aggregates size distribution in several models. In most cases, they behaved as a power-law with the diffusion length q or growth time t (or coverage) in some model parameters range. Here, the diffusion length is defined by the ratio:

$$q = \nu.\exp(-E_p/k_BT)/F, \tag{8}$$

where E_p is associated to the fastest diffusion process (in the dynamics) that sets the time scale. Values of q obtained for Pt(110) at

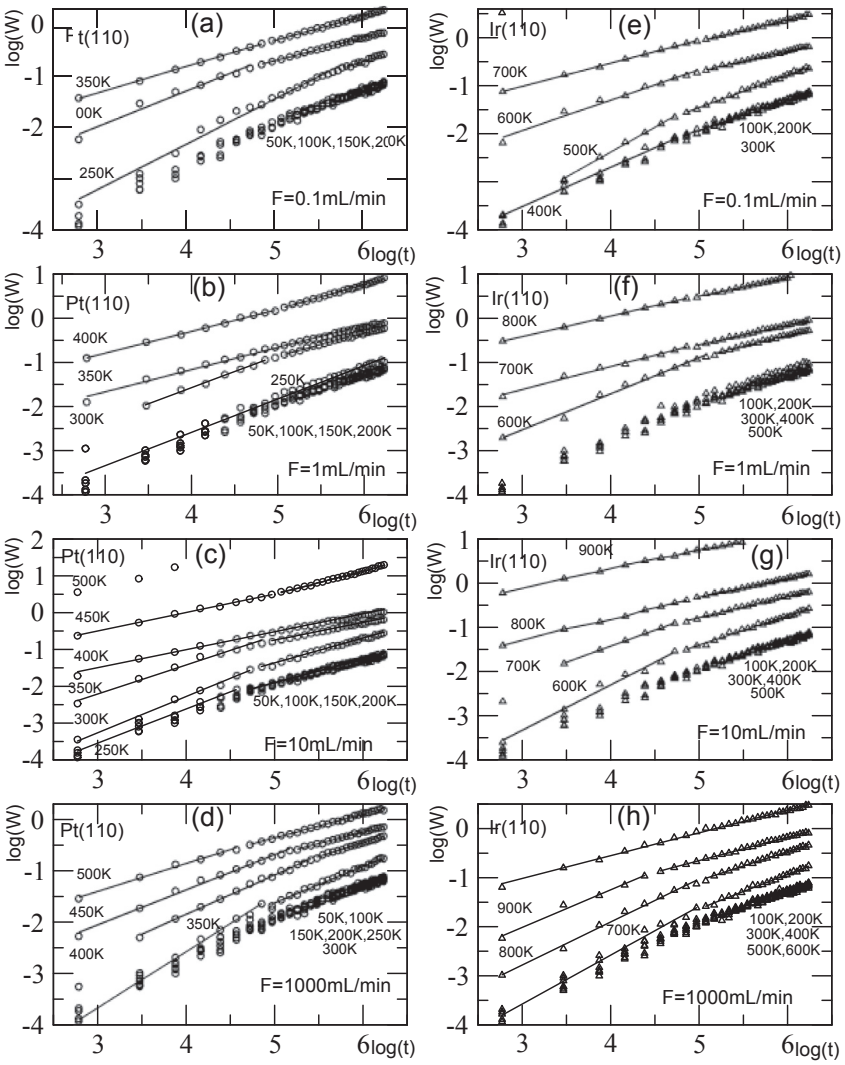

Fig. 4. Step widths as functions of growth time for Pt(110) surface (left panels) and Ir(110) surface (right panels) at selected temperatures and atom deposition fluxes in a log-log scale. Most curves show two linear and distinct trends separated by a short crossover region. Results suggest that the kinetic roughening of steps follows a power-law behavior at least at low coverages.

temperature T are almost the same for Ir(110) at temperature 2T. If the dependence on q obtained on high-symmetry surfaces for monomer and island densities holds on sloped surfaces, these quantities for Pt(110) and Ir(110) surfaces should behave similarly on q, at least in some parameters range. To check that, we plotted in Fig.5a,b computated values for both quantities as functions of the diffusion length q at constant atomic flux. Full signs are for Ir(110) while open signs are associated to Pt(110). In a wide range of small values of q, Na is a constant. Nc displays this feature for a coverage of 512 atoms deposited. For fewer atoms, it shows a slight decrease followed by an increase to a maximum. Decay of Na and Nc is observed from this maximum in a narrow q region. It is only there that power-law behavior with q could be shown. Beyond, computated data show important fluctuations. By analyzing values of Na and Nc at fixed and small q, the same increment is observed when the number of deposited atoms is doubled. This behavior observed on a log-log scale means that a power-law behavior exists for both quantities when plotted as functions of the real simulation time t. For credibility, we plotted in Fig. 5c both Na and N_c at T = 200K for Pt(110) and T = 400K for Ir(110). Both curves coincide. N_c displays three regimes with three different slopes. The latters can be related to the two onset temperatures defined above for each (110) surface. For the three regimes, we got the power-law exponents: 0.625(1); 2.324(2) and 1.722(3). For N_a, two regimes are visible with slopes: 0.913 and 0.594. When the temperature is raised (Fig.5d) to T = 300K for Pt(110) and T = 600K for Ir(110), other trends are recovered. $N_c(t)$ becomes linear with t. The adatom densities increase, pass by a maximum and then slowly decrease and no more power-law trend with t is expected. Let us remark that the coincidence observed at T = 200K and T = 400K in Fig.5c for Pt(110) and Ir(110) respectively failed. This means that other diffusion processes are becoming relevant in the whole dynamics. More computations are needed to fully substantiate all these pictures and to investigate the dependence of all results achieved here on surface slope u.

4. Conclusion

In this work, we studied the kinetic roughening of steps on Pt and Ir (110) surfaces by numerical simulations. The steps on both metal surfaces are characterized by their width. The behavior of this width with temperature suggests the existence of two onset

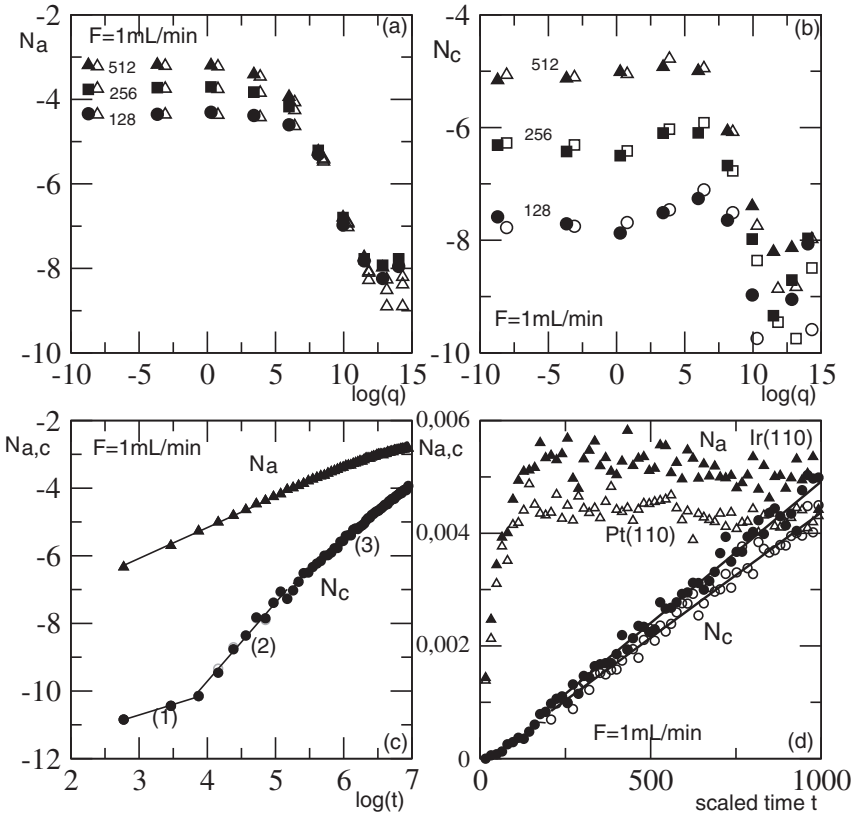

Fig. 5. Adatom (N_a) and island (N_c) densities as functions of growth time t and diffusion length q (see text). In panel (a), full signs are associated to Ir(110) surface at T = 400K while open signs are for Pt(110) surface at T = 200K. Results show that the adatom density at low coverage, fixed and small diffusion length, increases with the growth time. In panel (b), the same trend is observed for N_c. In panel (c), data are presented and coincide for the Pt (110) surface at T = 200K (open signs) and the Ir(110) surface at T = 400K (full signs). In panel (d), calculations made in panel (c) are performed in the case of T = 300K for Pt (110) and T = 600K for Ir(110). The power-law behavior got in panel (c) for both N_a and N_c is not suspected.

Table 3
Fitted values of exponent β for P t(100) and Ir(100) surfaces.

Surface	T (*K*)	*β*
Pt(110)	350	1.09 ± 0.02
	400	0.766 ± 0.014
	450	0.68 ± 0.02
	500	0.54 ± 0.02
Ir(110)	700	0.99 ± 0.05
	800	0.88 ± 0.03
	900	0.76 ± 0.05
	1000	0.465 ± 0.005

Table 4
Fitted values of the time exponent β for P t(110) and Ir(110) surfaces.

Surface	T (*K*)	F (*mL/min*)	*β*
Pt(110)	350	0.1	0.510 ± 0.006
		1	0.51 ± 0.01
		10	0.79 ± 0.04
		1000	1.09 ± 0.02
Ir(110)	700	0.1	0.485 ± 0.005
		1	0.52 ± 0.02
		10	0.734 ± 0.025
		1000	0.99 ± 0.05

temperatures. The first one is related to the relevance of surface diffusion in the dynamics and the second one is associated to reversible aggregation, ie to atom detachment events from steps or islands. At fixed temperature, the trend of steps width suggests that in the course of the time, interesting scaling behavior may be found. We checked that at several temperatures and selected deposition fluxes and discovered a power-law behavior of the step width with growth time. In the presence of simple relaxation, the trend is quite complicated and may be described by a combination of a logarithmic and a power functions. We also investigated monomer and island densities. At very low temperature, values of these quantities show a power-law behavior with growth, eg. at 200K for Pt and 400K for Ir (110). At small diffusion lengths, values of these quantities are constant. There exists an onset value of the diffusion length q from which they start to decrease. In this decay region, a power-law dependence of both quantities on q is suspected for larger coverages.

References

[1] A.L. Barabasi, H.E. Stanley, Fractal Concepts in Surface Growth, Cambridge University Press, Cambridge, 1995.
[2] D.E. Wolf, J. Villain, Europhys. Lett. 13 (1990) 389.
[3] S. Das Sarma, P.I. Tamborenea, Phys. Rev. Lett. bf 66 (1991) 325.
[4] G. Ehrlich, F.G. Huda, J. Chem. Phys. 44 (1966) 1039.
[5] R.L. Schwoebel, E.J. Shipsey, J. Appl. Phys. 37 (1999) 3682.
[6] G. Rosenfeld, R. Servanty, Ch Teichert, B. Poelsema, G. Comsa, Phys. Rev. Lett. 71 (1993) 895.
[7] K. Bromann, H. Brune, H. Roeder, K. Kern, Phys. Rev. Lett. 75 (1995) 677.
[8] M.D. Johnson, C. Orme, A.W. Hunt, D. Graff, J. Sudjidono, I.M. Sander, B.G. Orr, Phys. Rev. Lett. 72 (1994) 116.
[9] F. Starrost, E.A. Carter, Surf. Sci. 500 (2002) 323.
[10] F. Rosei, R. Rosei, Surf. Sci. 500 (2002) 395.
[11] K. Barnham, D. Vvedensky, Low-dimensional Semi-conductor Structures: Fundamentals and Device Applications, Cambridge University Press, Cambridge, 2001.
[12] F. Hontinfinde, M. Touzani, Surf. Sci. 338 (1995) 236.

[13] H.-C. Jeong, E.D. Williams, Surf. Sci. Rep. 34 (1999) 179.
[14] H. Ibach, Surf. Sci. Rep. 29 (1997) 193.
[15] R. Heid, R.K. Bohnen, A. Kara, T.S. Rahman, Phys. Rev. B 65 (2002) 115405.
[16] H.L. Richards, S.D. Cohen, T.L. Einstein, M. Giesen, Surf. Sci. 453 (2000) 59.
[17] C. Mottet, R. Ferrando, F. Hontinfinde, A.C. Levi, Surf. Sci. 417 (1998) 220.
[18] U.T. Ndongmouo, F. Hontinfinde, R. Ferrando, Phys. Rev. B 72 (2005) 115412.
[19] R. Ferrando, F. Hontinfinde, A.C. Levi, Phys. Rev. B 56 (1997) 4406.
[20] U.T. Ndongmouo, F. Hontinfinde, Surf. Sci. 571 (2004) 89.
[21] V. Rosato, M. Guillopé, B. Legrand, Phil. Mag. A 59 (1989) 321. M. Guillopé and B. Legrand, Surf. Sci. 215 (1989) 577.
[22] F. Montalenti, R. Ferrando, Phys. Rev. B 58 (1998) 3617.
[23] S. Rusponi, C. Boragno, R. Ferrando, F. Hontinfinde, U. Valbusa, Surf. Sci. 440 (1999) 451.
[24] F. Hontinfinde, R. Ferrando, Phys. Rev. B 63, (2001) 121403.
[25] A. B. Bortz, M. H. Kalos, J. L. Lebowitz, J. Comput. Phys. 17 (1975) L733.
[26] S.I.V. Hontinfinde, A.B. Akpo, F. Hontinfinde, Eur. Phys. J. (August 1st, 2016).
[27] J.A. Venables, G.D. Spiller, M. Hanbuecken, Rep. Prog. Phys. 47 (1984) 399.
[28] P. Jensen, H. Larralde, A. Pimpinelli, Phys. Rev. B 55 (1997) 2556.